# Aminophylline: thermal characterization and its inhibitory properties for the carbon steel corrosion in acidic environment

Adriana Samide · B. Tutunaru · Catalina Ionescu ·
P. Rotaru · Luminita Simoiu

**Abstract** Aminophylline (AMF) was studied as corrosion inhibitor for carbon steel in 1.0 mol $L^{-1}$ HCl solution using electrochemical measurements associated with UV–Vis spectrophotometry and optical microscopy. Simultaneous thermogravimetry/derivative thermogravimetry and differential scanning calorimetry analysis was performed in order to determine the temperature range in which AMF is an effective inhibitor, without the decomposition risk that could change the inhibition mechanism. Thermal behaviour restricts AMF application as corrosion inhibitor for carbon steel in 1.0 mol $L^{-1}$ HCl solution at temperatures ≤45 °C where there are no significant modifications of the adsorption mechanism. According to the results of electrochemical measurements, in association with UV–Vis spectrophotometry and optical microscopy techniques, AMF is a mixed-type inhibitor for carbon steel corrosion in 1.0 mol $L^{-1}$ HCl solution, simultaneously suppressing the anodic and cathodic processes and acting via spontaneous physisorption on the metal surfaces.

**Keywords** Pharmaceutical product · Thermal behaviour · Corrosion inhibition · Carbon steel · Electrochemical measurements

A. Samide (✉) · B. Tutunaru · C. Ionescu · L. Simoiu
Department of Chemistry, Faculty of Mathematics and Natural Sciences, University of Craiova, 107i Calea Bucuresti, 200512 Craiova, Romania
e-mail: samide_adriana@yahoo.com

P. Rotaru
Department of Physics, Faculty of Mathematics and Natural Sciences, University of Craiova, 13 AI Cuza Street, 200585 Craiova, Romania

## Introduction

The corrosion inhibition is a subject of intense research for many scientific and industrial applications where the mass reduction of different metals could be avoided by the improvement of their corrosion resistance using effective methods to protect the underlying substrate surface.

Hydrochloric and sulphuric acid solutions are widely used in industry, notable applications including the cleaning and pickling of steel [1, 2]. Because of the general aggression effect of these solutions, the corrosive attacks on metallic surfaces are promoted.

Mass loss measurements, voltammetric techniques and electrochemical impedance spectroscopy have been used to evaluate the corrosion resistance of steel in aqueous acid solutions [3–5]. Since the structure life of steel is often influenced by the surface corrosion, the composition and thermal behaviour of the rust formed on the steel surface is of great interest. The thermal analysis method has been applied by several workers for the study of the iron corrosion products resulted in both uninhibited and inhibited solutions [6–9], and to characterize some organic compounds with applications in various fields [10–16].

The use of inhibitors is the most appropriate way to isolate the metal from corrosive agents and thus to reduce corrosion reactions [17, 18]. The inhibitors are organic molecules containing nitrogen, oxygen and/or sulphur as electron donating heteroatoms, or heterocyclic molecules with π-orbitals. The inhibition efficiency of these compounds depends on their ability to be adsorbed on the metallic surface. The toxic effects of most synthetic inhibitors and the obligations to respect the norms of human health and safety have lead to the research of green alternatives, and several eco-friendly and harmless inhibitors have been reported [18–44].
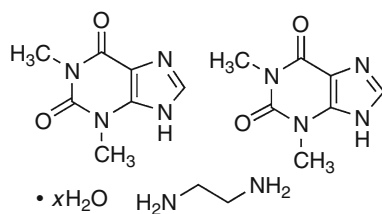
**Fig. 1** Molecular structure of AMF

Recently, several studies have been carried out on the inhibition of steel corrosion by the natural extracts of *Asteriscus graveolens* [18], *Jatropha curcas* [19], *Phyllanthus amarus* [20], *Sesamum indicum* [21], *Chenopodium ambrosioides* [22], *Foeniculum vulgare* [23], *Xylopia ferruginea* [24], *Murraya koenigii* [25], *Eugenia jambolana* [26], *Zenthoxylum alatum* [27], *Simiria tinctoria* and *Guatteria ouregou* [28], *Oxandra asbeckii* [29], *Aloe vera* [30], *Moringa oleifera*, *Piper longum* and *Citrus aurantium* [31], *Ginkgo* [32], *Haematoxylum campechianum* [33], apricot juice [34] and caffeic acid [35].

Survey of the literature reveals that many pharmaceutical active compounds have been evaluated as effective green corrosion inhibitors for different metals: Ampicillin [36], Amoxycillin [37], Cefalexin [38], Cip rofloxacin [39], Norfloxacin [40], Doxycicline [41], Erythromycin [42], Sulfacetamide [43] and Streptomycin [44].

The aim of the present study is to investigate the thermal behaviour of aminophylline in order to establish the temperature range where its stability is observed to be recommended as a corrosion inhibitor, without decomposition risk, for carbon steel in 1.0 mol $L^{-1}$ HCl solution. The results of thermal analysis were illustrated by the thermoanalytical (TG/DTG/DSC) curves. The inhibitory and adsorption properties of AMF were studied using electrochemical measurements, followed by UV–Vis spectrophotometry and optical microscopy techniques. Aminophylline (AMF) is a pharmaceutical product containing theophylline (THP) and ethylenediamine (EDA) in ratio of 2:1 being known under the following synonyms: (Theophylline)$_2$Ethylenediamine; 3,7-Dihydro-1,3-dimethyl-1H-purine-2,6-dione, compound with 1,2-ethanediamine (2:1). Theophylline hemiethylenediamine complex is a bronchodilator drug that is usually found as a monohydrate or dihydrate. The molecular structure of AMF is presented in Fig. 1.

**Experimental**

Materials

The thermal behaviour and inhibitory properties of AMF, a Sigma-Aldrich powder (assay ≥98.0 %; impurity

~1 mol/mol H$_2$O), were investigated. The preliminary thermal study of EDA (liquid compound) was performed using a Sigma-Aldrich product (assay ≥99.5 %; vapour density versus air of 2.07; vapour pressure of 1.3 kPa at 20 °C). The plates of carbon steel (area 1.0 cm$^2$) with the following composition (mass%): C = 0.1; Si = 0.035; Mn = 0.4; Cr = 0.3; Ni = 0.3; and Fe the remainder until 100 %, were used as working electrodes during the electrochemical measurements. The samples were mechanically polished with emery paper, degreased with acetone and dried in warm air. The corrosion tests were performed in 1.0 mol $L^{-1}$ HCl (AR—obtained from Merck) blank solution and in 1.0 mol $L^{-1}$ HCl solutions containing various concentrations of AMF: 0.2; 0.4 and 0.6 mmol $L^{-1}$.

Methods and techniques

*Thermal analysis*

The thermal analysis of AMF was performed in nitrogen atmosphere using a Diamond analyzer from Perkin-Elmer with Pyris software. The sample (3.02 mg) was heated in alumina crucibles in the temperature range of *RT*-400 °C, with a heating rate of 10 °C min$^{-1}$. Moreover, ethylenediamine (EDA) thermal behaviour was studied by heating of 1.7 mg in the temperature range of *RT*-200 °C, with a heating rate of 10 °C min$^{-1}$. The dynamic conditions were achieved by N$_2$ gas purging with a constant flow of 150 mL min$^{-1}$.

*Electrochemical measurements*

The potentiodynamic polarization and the measurements of polarization resistance in time were used to determine the corrosion current density and degree of surface coverage (θ) for carbon steel corroded in 1.0 mol $L^{-1}$ HCl blank solution and in 1.0 mol $L^{-1}$ HCl solution containing various concentration of AMF: 0.2; 0.4 and 0.6 mmol $L^{-1}$. All the electrochemical measurements were carried out using a VoltaLab 40 potentiostat/galvanostat, with Volta-Master 4 software. The experiments were performed using a glass corrosion cell with three electrodes: a platinum auxiliary electrode, a saturated Ag/AgClsat reference electrode and the carbon steel sample as working electrodes. The immersion time of the plates in the aggressive media was 4.0 min in open circuit, at room temperature. The polarization curves were recorded with a scan rate of 1.0 mV s$^{-1}$.

*UV–Vis spectrophotometry*

The samples of 1.0 mol $L^{-1}$ HCl solution containing various concentrations of AMF above mentioned were used

**Fig. 2** Thermoanalytical curves of EDA
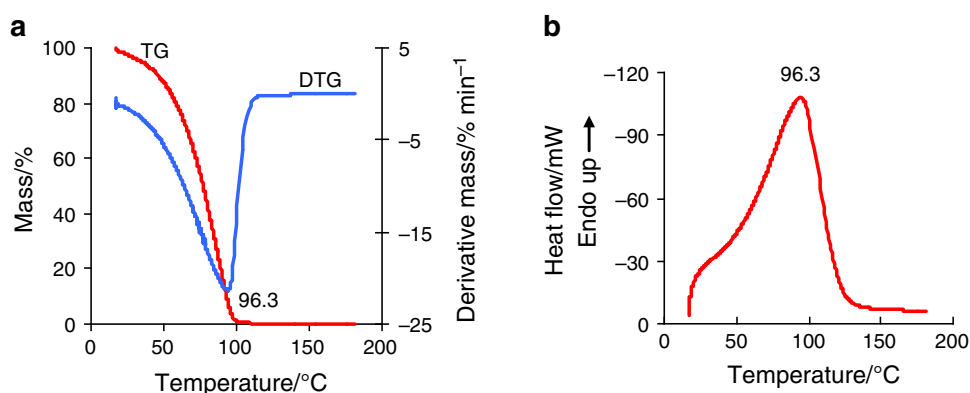


for spectrophotometric analysis, before and after the potentiodynamic polarization. UV–Vis analysis reports were obtained using a UV–Vis spectrophotometer, Varian-Cary 50 type, with Cary WinUV software.

*Surface characterization*

The surface morphologies of the carbon steel electrodes, before and after corrosion in 1.0 mol L$^{-1}$ HCl solution and in 1.0 mol L$^{-1}$ HCl solution containing various concentrations of AMF, were examined using a metallographic microscope, type Euromex with Canon camera and included ZoomBrowser—EOS Digital software.

## Results and discussion

Thermal analysis

In order to recommend AMF as a corrosion inhibitor, its thermal stability was studied according to the decomposition levels which have been illustrated on the TG curve accompanied by the DTG/DSC curves. A preliminary study of thermal analysis of EDA was performed, knowing that AMF contains this compound. The results are illustrated in Fig. 2 which shows the TG/DTG (Fig. 2a) and the DSC (Fig. 2b) curves obtained in the temperature range from RT to 180 °C. It can be observed that the TG curve presents a single step of mass loss that corresponds to one peak on DTG centred at 96.3 °C. This is followed by one endothermic peak, reaching a maximum at 96.3 °C on the DSC curve. This thermal behaviour is attributed to the evaporation process of EDA, starting at 40 °C and ending until 116 °C.

The thermal analysis of AMF, performed in temperature range from RT to 400 °C, is presented in Fig. 3. On TG/DTG curves (Fig. 3a) four distinctive steps of AMF decomposition are noticed, accompanied by four endothermic peaks on DSC curve (Fig. 3b) observed at the same temperature. For a more accurate observation of the

temperature ranges where major changes of mass loss takes place, TG/DSC curves were detailed in the range of low temperatures up to 200 °C, and at high temperatures between 200 and 400 °C.

As shown in Fig. 3c, at low temperatures, three mass loss steps are observed: (i) between 40 and 117 °C, the mass loss of 7.46 % is attributed to EDA evaporation; the corresponding peak on DTG curve, and the endothermic peaks on DSC curves (Fig. 3b, c) at 96.3 °C indicate a similar process of EDA evaporation as that shown in Fig. 2. The observed mass loss is less than that expected (13.69 %) for the loss of 1 mole of EDA. The results indicate an incomplete evaporation, and suggest that a part of EDA molecules are superficially adsorbed [45] on the surface of AMF powder, and the other is intercalated, being blocked among theophylline (THP) molecules, and/or these are strongly linked inside of AMF particles; (ii) the second endothermic process at 126.1 °C, accompanied by a mass loss of 3.83 %, in the temperature range from 117 to 145 °C, is also slightly smaller than the expected mass loss (4.1 %) corresponding to 1 mole of water and (iii) between 145 and 175 °C, the TG curve shows a sharp drop (mass loss of 6.49 %) accompanied by the endothermic peak which can probably be assigned to the decomposition of linked EDA which could be fragmented as $N_2/C_2H_4$, $NH_3$ and $H_2$ [46]. However, it is difficult to strictly connect the values of the temperature ranges with the independent processes related to EDA evaporation, or decomposition, and AMF dehydration. It is possible that parallel courses of these processes take place, and the occurrence of overlapping phenomenon cannot be excluded. It is certain that until the temperature of 175 °C, the mass loss is 17.68 %, meaning that this stable mixture of theophylline and ethylenediamine decomposes at low temperatures with dehydration of one molecule of crystallization water and evaporation of one molecule of EDA. This is in good agreement with the expected (17.8 %) loss of ~1.0 mol of water and 1.0 mol of EDA. Similar results were obtained for AMF dihydrate [47, 48].

**Fig. 3** Thermoanalytical curves of AMF detailed as **a** TG/DTG curves, **b** DSC curve, **c** TG/DSC curves of decomposition steps at low temperatures and **d** TG/DSC curves decomposition steps at high temperatures
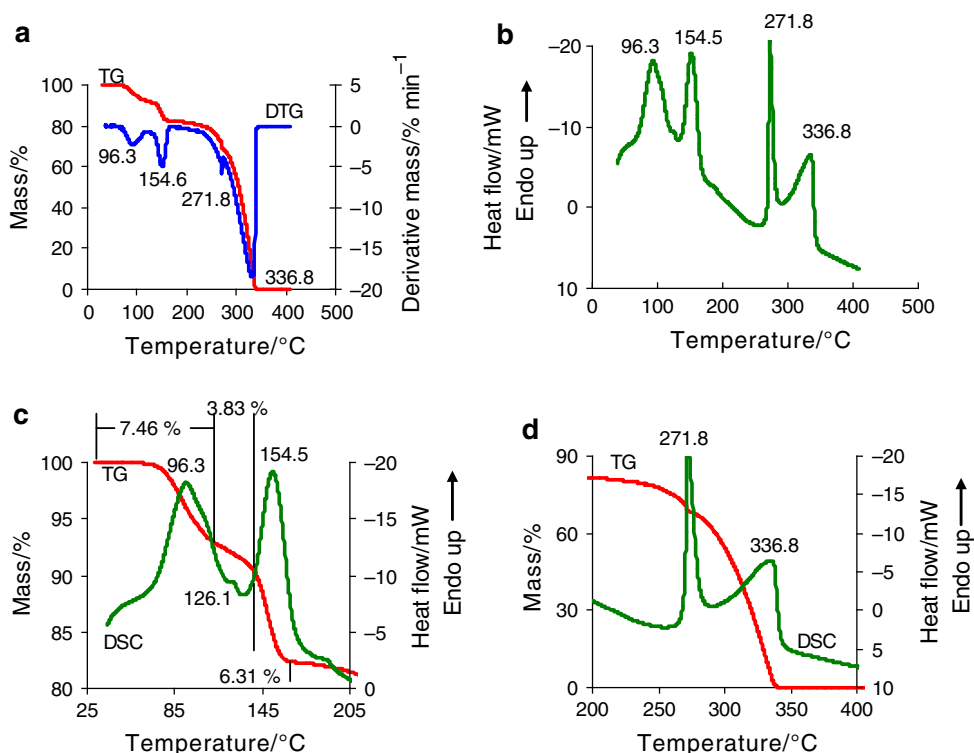


**Table 1** Ranges of temperatures, media and potential risks related to the use AMF as corrosion inhibitor

| Temp./°C | Medium | Composition THP; EDA/mole AMF | | Risks |
|---|---|---|---|---|
| | | THP | EDA | |
| <45 | Aqueous | 2.0 mol | 1.0 mol | No risk |
| 45–75 | Aqueous | 2.0 mol | <1.0 mol | Gradual and uncontrolled release of EDA |
| 75–100 | Aqueous | 2.0 mol | Far less than 1.0 mol | Change of inhibition mechanism; this should prevailing discussed in relation to THP |
| 100–250 | Organic heat-transfer agents | <2.0 mol | – | Change of inhibition mechanism; gradual and uncontrolled release of THP |
| >250 | – | – | – | Not suitable |

The TG/DSC curves of AMF obtained at high temperatures are presented in Fig. 3d. TG/DSC curves detailed at high temperatures are assigned to theophylline thermal behaviour. An inflection on the TG curve can be seen at 271.8 °C accompanied by an endothermic peak on the DSC curve, at the same temperature. Thus, until this temperature, other processes could occur such as elimination of water, and other gases resulted from the EDA decomposition, and/or THP begins to sublimate [49], and its melting point being at 271.8 °C [47, 48]. Then, THP evaporates up to 337 °C with minimal residue. Based on these data, certain recommendations are necessary in order to use AMF as corrosion inhibitor for some metals in different media. The possible risks which might occur in the process of inhibition are presented in Table 1.

### AMF inhibitory properties

*Potentiodynamic polarization*

The potentiodynamic polarization was performed with a scan rate of 1.0 mV s$^{-1}$ in 1.0 mol L$^{-1}$ HCl blank solution and in 1.0 mol L$^{-1}$ HCl solution containing various concentrations of AMF: 0.2; 0.4 and 0.6 mmol L$^{-1}$, after the carbon steel electrode prepolarization in open circuit for 10 min at room temperature. The UV–VIS scans were

**Fig. 4** Polarization anodic and cathodic curves obtained for carbon steel corroded in 1.0 mol L$^{-1}$ HCl blank solution and in 1.0 mol L$^{-1}$ HCl solution containing various concentrations of AMF, at room temperature (**a**); UV–Vis scans obtained for various AMF concentrations in 1.0 mol L$^{-1}$ HCl solution, before and after potentiodynamic polarization (**b**)
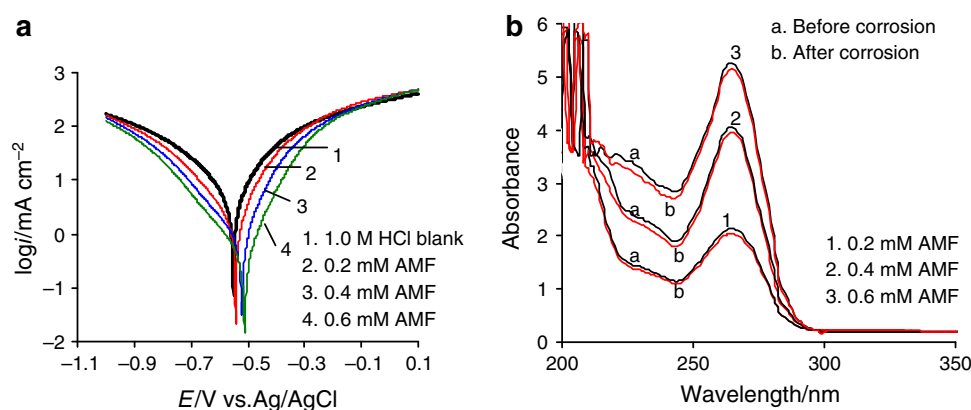


recorded for inhibited 1.0 mol L$^{-1}$ HCl solution with different AMF concentrations, before and after corrosion, in order to discuss the AMF electrochemical stability. Figure 4 presents the potentiodynamic curves (Fig. 4a) and UV–Vis scans (Fig. 4b) obtained in given laboratory conditions.

From Fig. 4a, it can be observed that the presence of AMF in 1.0 mol L$^{-1}$ HCl solution causes the following transformations on the polarization curves:

– the corrosion potential ($E_{corr}$) was shifted to higher values, while the polarization curves have been shifted to lower current regions. These phenomena certify the inhibition tendency of this compound that is more obvious with increasing of its concentration in hydrochloric acid solution;
– both cathodic (hydrogen evolution) and anodic (carbon steel dissolution) reactions were simultaneously inhibited in the same manner;
– the cathodic curves give approximately parallel lines, suggesting that the hydrogen discharge reaction lowers, its activation being controlled [50, 51] by AMF addition in aggressive medium; and
– in the vicinity of $E_{corr}$, an appreciable decrease in the current density is observed starting with the concentration of 0.2 mmol L$^{-1}$ AMF, suggesting the formation of an anodic protective layer on the carbon steel surface [51].

Based on these observations it can be concluded that AMF acts as a mixed-type inhibitor by forming a protective layer, as an effective barrier which interposes to electrode/medium interface, suppressing the metal ionization. In previous studies [51–53], a similar behaviour for other pharmaceutical products was reported. All the phenomena previously described indicate that the corrosion current ($i_{corr}$) values decrease with the increase of AMF concentration. The corrosion current ($i_{corr}$) was calculated by extrapolation of anodic and cathodic Tafel lines to corrosion potential ($E_{corr}$) using VoltaMaster 4 software.

**Table 2** Electrochemical parameters and inhibition efficiency (IE) obtained from Tafel polarization for carbon steel corroded in 1.0 mol L$^{-1}$ HCl solution in the absence and in the presence of various concentrations of AMF, at room temperature

| $C$-AMF/ mmol L$^{-1}$ | $E_{corr}$/V vs. Ag/AgCl | $i_{corr}$/ mA cm$^{-2}$ | $b_a$/ mV dec$^{-1}$ | $b_c$/ mV dec$^{-1}$ | IE/ % |
|---|---|---|---|---|---|
| 0 | −0.55 | 2.83 | 103 | 135 | 0 |
| 0.2 | −0.542 | 1.17 | 86 | 130 | 58.6 |
| 0.4 | −0.522 | 0.63 | 81 | 141 | 77.8 |
| 0.6 | −0.512 | 0.36 | 87 | 145 | 87.3 |

The electrochemical parameters such as the corrosion potential ($E_{corr}$), corrosion current density ($i_{corr}$), anodic and cathodic Tafel slopes ($b_a$ and $b_c$), as well as the inhibition efficiency (IE), as a function of AMF concentration ($C$-AMF) are given in Table 2. The inhibition efficiency percentage (IE) of AMF was determined from polarization measurements according to Eq. 1 [51–53]:
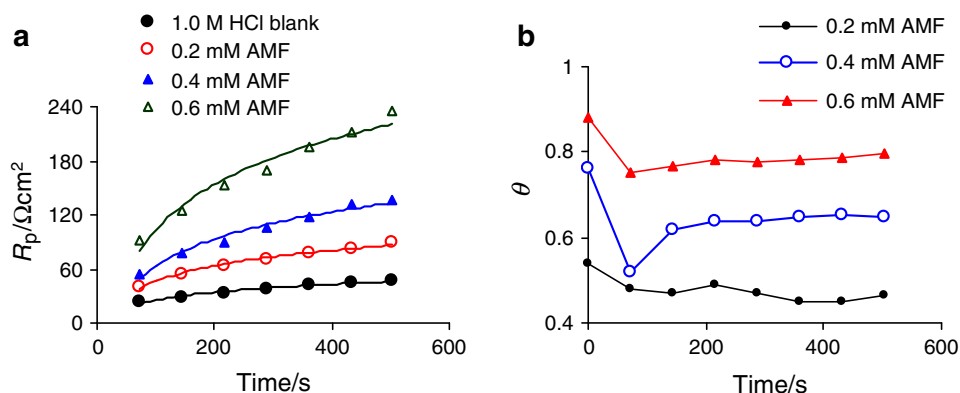
$$IE = \frac{i_{corr}^{o} - i_{corr}}{i_{corr}^{o}} \times 100 \qquad (1)$$

where $i_{corr}^{o}$ and $i_{corr}$ are the corrosion current densities of carbon steel in 1.0 mol L$^{-1}$ HCl solution without and with AMF, respectively.

From Table 2, it can be observed that (i) with the increase in AMF concentration, $i_{corr}$ values gradually decrease; (ii) the anodic ($b_a$) and cathodic ($b_c$) Tafel slopes are slightly changed after the inhibitor addition and (iii) this indicates that AMF influences the anodic and cathodic processes, and consequently, the inhibition efficiency (IE) increases with AMF concentration, reaching a maximum value of 87.3 % at 0.6 mmol L$^{-1}$ AMF in 1.0 mol L$^{-1}$ HCl solution.

To study the electrochemical stability of AMF, as well as its adsorption capacity on carbon steel surface, UV–Vis spectra of studied solutions, before and after corrosion processes, were performed. Figure 4b illustrates the UV–Vis scans obtained for the studied AMF concentrations

before and after potentiodynamic polarization. From Fig. 4b, it can be observed that the UV–Vis spectra of the AMF show one intense band at 270 nm. A similar result was obtained for AMF in water [54], the difference consisting in a slightly alteration of wavelength from 271 [54] to 270 nm. After corrosion, it can be observed that AMF absorbance slightly decreases without altering the wavelength of adsorption maximum, and consequently the inhibitor concentration in corrosive medium follows the same trend. A very small decrease in the AMF concentration suggests that an adsorption process of the organic compound from aqueous phase on the electrode surface may occur.

*AMF action mechanism*

In order to discuss the AMF film stability, the variation of polarization resistance ($R_p$) in time was recorded. Moreover, the degree of surface coverage ($\theta$) values were calculated using Eq. 2, and consequently the inhibition efficiency (*IE*) will be determined as $\%IE = 100 \cdot \theta$ [50, 51, 53, 54].

$$\theta = \left( \frac{R_p - R_p^o}{R_p} \right) \qquad (2)$$

where $R_p$ and $R_p^o$ represent the polarization resistance at a given time in the presence and in the absence of AMF, respectively.

The variations of $R_p$ and $\theta$ in time are both shown in Fig. 5.

From Fig. 5a, it is observed that the increase of polarization resistance in time becomes much more obvious at high AMF concentrations. This suggests that AMF acts by adsorption on carbon steel surface and that the mechanism of inhibitor film formation is tightly linked to the AMF concentration. Moreover, it can be estimated that the adsorption process of AMF molecules on carbon steel surface prevails over the desorption phenomenon. The

same trend is also observed for the degree of surface coverage ($\theta$), excepting the first moments which mark a relatively sharp decrease of its values (Fig. 5b). This could be explained by the presence of some anodic areas on the carbon steel surface, where corrosion processes are relatively intense, inducing instability and permeability to inhibitor film. At the concentration of 0.2 mmol L$^{-1}$ AMF, the fluctuations of $\theta$ values persist, which means that the inhibitor concentration is too low to ensure the formation of a continuous and somewhat compact layer to protect the metal surface. For the concentrations higher than 0.2 mmol L$^{-1}$, it is observed that $\theta$ values are stable reaching an average value of 0.65 at an AMF concentration of 0.4 mmol L$^{-1}$ and 0.8 for 0.6 mmol L$^{-1}$ AMF, respectively. Consequently, *IE* reaches the values of 65, and 80 %, respectively, and these being slightly different from those obtained from potentiodynamic polarization. This difference is predictable because in the given conditions, the inhibitor film carries out several cycles of adsorption–desorption of AMF molecules from carbon the steel surface until concretization of its texture. Based on Freundlich adsorption isotherm [55], Eq. 3 could be used, as a possible relationship between $\theta$ and AMF concentration, in the range where $\theta$ has a constant value:

$$\theta = K \cdot C^n, \qquad (3)$$

where *K is* the equilibrium constant of adsorption–desorption (*K*), *C* is the AMF concentration, *n* is a heterogeneous factor of metal surface and 1/*n* representing the number of surface active sites occupied by one inhibitor molecule.

Equation 3 can be also written in the following form, Eq. 4:

$$\ln \theta = \ln K + n \ln C \qquad (4)$$

Thus, taking into consideration these observations, the following system of equations can be used to determine *K* and *n*:

**Fig. 6** The microscopic images of carbon steel surfaces **a** before corrosion, **b** after corrosion in 1.0 mol $L^{-1}$ HCl blank solution, **c** after corrosion in 1.0 mol $L^{-1}$ HCl solution containing 0.4 mol $L^{-1}$ AMF and **d** after corrosion in 1.0 mol $L^{-1}$ HCl solution containing 0.6 mol $L^{-1}$ AMF
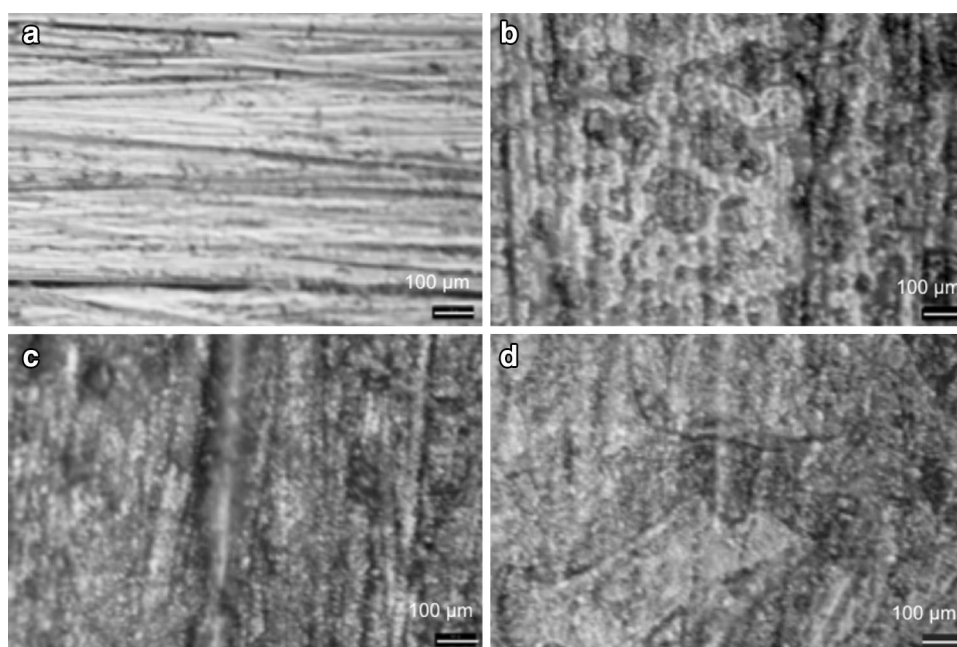


$$\ln \theta_1 = \ln K + n \ln C_1 \qquad (5)$$

$$\ln \theta_2 = \ln K + n \ln C_2 \qquad (6)$$

where $\theta_1 = 0.65$, $\theta_2 = 0.8$, $C_1 = 4 \times 10^{-4}$ mol $L^{-1}$ and $C_2 = 6 \times 10^{-4}$ mol $L^{-1}$.

The equilibrium constant of adsorption–desorption ($K$) process was used to calculate the free energy of adsorption ($\Delta G^o_{ads}$) using Eq. 7 [50–52, 55]:

$$\Delta G^o_{ads} = R \cdot T[\ln(1/55.5) - \ln K] \qquad (7)$$

where $R$ is the universal constant of gases (8.31 J $mol^{-1}$ $K^{-1}$), $T$ is the temperature (298 K) and 55.5 is the value of the molar concentration of water in the solution, $\ln K = 3.58$.

The calculated value for $\Delta G^o_{ads}$ around of $-19.0$ kJ $mol^{-1}$ (consequently, binding energy value of AMF molecule at carbon steel surface of 0.19 eV) is consistent with the electrostatic interaction between the charged molecules and the charged metal surface and/or different H–, Cl–, bridges or Van der Waals bonds (physical adsorption) [56, 57]. This result also shows that the adsorption of AMF molecules on the metal surface is a spontaneous process. To note that, the $\Delta G^o_{ads}$ value was calculated taking into account two concentrations of AMF inhibitor where constant values for $\theta$ were obtained; considering that, in these cases only, adequate amounts of inhibitor there are to form the stable and uniform layers and consequently, the adsorption process prevails on the desorption one. Although, it could be appreciated as a relative value, not so reliable, $-19.0$ kJ $mol^{-1}$ is indicative for the adsorption of AMF molecules, this being higher than $-40.0$ kJ $mol^{-1}$ that is usually accepted as a

threshold value between chemical and physical adsorption [50, 51, 55].

The result obtained for $1/n$ (around of 2.0 value) indicates that a single molecule of AMF disables several active sites from the metal surface [50].

The inhibition mechanism of AMF requires knowledge of inhibitor action at the electrode–solution interface. In acid solution, both THP and EDA can be in the protonated forms. The surface charge of carbon steel in HCl solution is known to be positive [56]. Thus, the Cl ions are adsorbed on metal surface generating excess negative charge towards the solution. This indicated that the electrostatic interactions of the protonated inhibitor molecules on the negatively charged metal surface are favoured. The adsorption of the AMF molecules can also occur on the mild steel surface by direct interaction of the lone pairs of electrons on nitrogen atoms and $d$-orbital of Fe [56]. The lone pairs of electrons of nitrogen atoms from EDA or imidazole ring of theophylline could also form complexes with $Fe^{2+}$ ions occurred from the anodic dissolution of carbon steel. Both EDA-metal as well as THP-metal complexes are known [58, 59]. Ethylenediamine forms a large number of complexes with many metal ions, including iron [58]. EDA usually acts as a monodentate or bidentate ligand, but this can also form the protonated complexes [58]. These complexes can adsorb onto the steel surface through Van der Waals bonds, and this is consistent with the binding energy value of 0.19 eV, attesting that the anchoring of these complexes at the carbon steel surface enhances the substrate protection against corrosion [59].

## Surface characterization

The microscopic images of carbon steel surfaces before and after the electrochemical measurements obtained in 1.0 mol L$^{-1}$ HCl blank solution and in 1.0 mol L$^{-1}$ HCl solution containing various concentrations of AMF are shown in Fig. 6. The characteristic morphology of the carbon steel surface before the corrosion process is observed in Fig. 6a. After the electrochemical measurements, carbon steel surface was coated with large corrosion spots which change its texture (Fig. 6b). This process is quite different compared to those obtained in the presence of AMF (Fig. 6c, d). The feature of the texture, which could be attributed to a protective layer on carbon steel surface, is nuanced, highlighting that the intensity of the corrosion spots decreases with increase in AMF concentration (Fig. 6c, d).

## Conclusions

Thermal analysis showed that at low temperatures, the following events occurred: (i) between 40 and 117 °C, the mass loss of 7.46 % was ascribed to EDA evaporation; (ii) 40 and 175 °C the mass loss of 10.22 % was assigned to the overlapped processes of EDA evaporation/decomposition and the elimination of hydration water, which simultaneously take place. Thus, AMF thermal instability restricts its application as corrosion inhibitor at high temperatures, indicating a confidence interval that does not exceed 45 °C.

The potentiodynamic polarization has indicated that AMF acts as a mixed-type inhibitor in 1.0 mol L$^{-1}$ HCl solution, simultaneously suppressing anodic and cathodic processes by formation of an adsorbed protective layer on carbon steel surface. The value around of −19.0 kJ mol$^{-1}$ obtained for $\Delta G^o_{ads}$ is consistent with the physical adsorption mechanism, and this also showing that the adsorption of AMF molecules on metal surface is a spontaneous process. A sinergic physical adsorption mechanism involving H–, Cl–, bridges and Van der Waals bonds via AMF complexes, which can provide the anchoring of inhibitor at carbon steel surface is supported by binding energy value of 0.19 eV obtained in this study.

The UV–Vis scans recorded for 1.0 mol L$^{-1}$ HCl solution containing the studied AMF concentrations indicated its high electrochemical stability by a slight decrease of absorbance after corrosion associated with adsorption process of inhibitor molecules from aqueous phase to electrode surface.

The optical microscopy, by comparative images, has indicated that the feature of protective layer on the carbon steel surface is nuanced.

## References

1. Sathiyanarayanan S, Marikkannu C, Palaniswamy N. Corrosion inhibition effect of tetramines for mild steel in 1 M HCl. Appl Surf Sci. 2005;241:477–84.
2. Trabanelli G. Inhibitors an old remedy for new challenge. Corrosion. 1991;47:410–9.
3. Gece G. Drugs: a review of promising novel corrosion inhibitors. Corros Sci. 2011;53:3873–98.
4. Kumar H, Karthikeyan S. Inhibition of mild steel in hydrochloric acid solution by cloxacillin drug. J Mater Environ Sci. 2012;3:925–34.
5. Vaszilcsin N, Ordodi V, Borza A. Corrosion inhibitors from expired drugs. Int J Pharm. 2012;431:241–4.
6. Samide A, Tutunaru B, Dobritescu A, Negrila C. Study of the corrosion products formed on carbon steel surface in hydrochloric acid solution. J Therm Anal Calorim. 2012;110:145–52.
7. Tutunaru B, Samide A, Negrila C. Thermal analysis of corrosion products formed on carbon steel in ammonium chloride solution. J Therm Anal Calorim. 2013;111:1149–54.
8. Thickett D, Odlyha M. Application of thermomagnetometry to corrosion studies of archaeological iron. J Therm Anal Calorim. 2005;80:565–71.
9. Rusu I, Sutiman D, Lisa G, Mareci D, Melniciuc Puica N. On the correlation between thermal analysis results and corrosion behaviour of some metallic religious artefacts. J Therm Anal Calorim. 2011;104:423–30.
10. Rotaru A, Moanţă A, Popa G, Rotaru P, Segal E. Thermal decomposition kinetics of some aromatic azomonoethers. Part IV. Non-isothermal kinetics of 2-allyl-4-((4-(4-methylbenzyloxy) phenyl)diazenyl) phenol in dynamic air atmosphere. J Therm Anal Calorim. 2009;97:485–91.
11. Rotaru A, Moanţă A, Rotaru P, Segal E. Thermal decomposition kinetics of some aromatic azomonoethers. Part III. Non-isothermal study of 4-[(4-chlorobenzyl)oxy]-4′-chloro-azobenzene in dynamic air atmosphere. J Therm Anal Calorim. 2009;95:161–6.
12. Rotaru A, Kropidłowska A, Moanţă A, Rotaru P, Segal E. Thermal decomposition kinetics of some aromatic azomonoethers. Part II. Non-isothermal study of three liquid crystals in dynamic air atmosphere. J Therm Anal Calorim. 2008;92:233–8.
13. Rotaru A, Moanţă A, Sălăgeanu I, Budrugeac P, Segal E. Thermal decomposition kinetics of some aromatic azomonoethers. Part I. Decomposition of 4-[(4-chlorobenzyl)oxy]-4′-nitro-azobenzene. J Therm Anal Calorim. 2007;87:395–400.
14. Rotaru A, Brătulescu G, Rotaru P. Thermal analysis of azoic dyes: part I. Non-isothermal decomposition kinetics of [4-(4-chlorobenzyloxy)-3-methylphenyl](p-tolyl)diazene in dynamic air atmosphere. Thermochim Acta. 2009;489:63–9.
15. Moanţă A, Tutunaru B, Rotaru P. Spectral and thermal studies of 4-(phenyldiazenyl)phenyl 2-furoate as corrosion inhibitor for carbon steel. J Therm Anal Calorim. 2013;111:1273–9.
16. Raja PB, Sethuraman MG. Natural products as corrosion inhibitor for metals in corrosive media—a review. Mater Lett. 2008;62:113–6.
17. Adamczyk L, Pietrusiak A, Bala H. Corrosion resistance of stainless steel covered by 4-aminobenzoic acid films. Cent Eur J Chem. 2012;10:1657–68.
18. Znini M, Cristofai G, Majidi L, Ansari A, Bouyanzer A, Paolini J, Costa J, Hammouti B. Green approach to corrosion inhibition of mild steel by essential oil leaves of Asteriscus Graveolens (Forssk.) in sulphuric acid medium. Int J Electrochem Sci. 2012;7:3959–81.
19. Vinod Kumar KP, Sankara Narayanan Pillai M, Rexin Thusnavis G. Inhibition of mild steel in hydrochloric acid by the seed husk extract of Jatropha curcas. J Mater Sci. 2010;1:119–28.
20. Sribharathy V, Rajendran S, Sathiyabama J. Inhibitory action of Phyllantus Amarus extract on the corrosion of mild steel in seawater. Chem Sci Trans. 2013;. doi:10.7598/cst2013.252.

21. Popoola API, Abdulwahab M, Fayomi OSI. Corrosion inhibition of mild steel in *Sesamum indicum*-2 M HCl/H$_2$SO$_4$ interface. Int J Electrochem Sci. 2012;7:5805–16.

22. Rodriguez-Clemente E, Gonzalez-Rodriguez JG, Valladarez G, Dominguez-Patino GF. Corrosion inhibition of carbon steel in H$_2$SO$_4$ by *Chenopodium ambrosioides*. Int J Electrochem Sci. 2011;6:6360–72.

23. Lahhit N, Bouyanzer A, Desjobert JM, Hammouti B, Salghi R, Costa J, Jama C, Bentiss F, Majidi L. Fennel (*Foeniculum vulgare*) essential oil as green corrosion inhibitor of carbon steel in hydrochloric acid solution. Portug Electrochim Acta. 2011;29:127–38.

24. Elyn Amira WAW, Rahim AA, Osman H, Awang K, Bothi Raja P. Corrosion inhibition of mild steel in 1 M HCl solution by *Xylopia ferruginea* leaves from different extract and partitions. Int J Electrochem Sci. 2011;6:2998–3016.

25. Quraishib MA, Singha A, Singha VK, Yadavb DK, Singh AK. Green approach to corrosion inhibition of mild steel in hydrochloric acid and sulphuric acid solutions by the extract of *Murraya koenigii* leaves. Mater Chem Phys. 2010;122:114–22.

26. Deepa rani P, Petchiammal A, Pirammarjeswari M, Rajeswari C, Selvaraj S. *Eugenia jambolana* used as corrosion inhibitor on mild steel in 1 N hydrochloric acid medium. Am J Phytomed Clin Therap. 2013;1:215–25.

27. Chauhan LR, Gunasekaran G. Corrosion inhibition of mild steel by plant extract in dilute HCl medium. Corros Sci. 2007;49:1143–61.

28. Lecante A, Robert F, Blandinieres PA, Roos C. Anti-corrosive properties of *S. tinctoria* and *G. ouregou* alkaloid extracts on low carbon steel. Curr Appl Phys. 2011;11:714–24.

29. Lebrini M, Robert F, Lecante A, Roos C. Corrosion inhibition of C38 steel in 1 M hydrochloric acid medium by alkaloids extract from *Oxandra asbeckii* plant. Corros Sci. 2011;53:687–95.

30. Sribharathy V, Rajendran S, Rengan P, Nagalakshmi R. Corrosion inhibition by an aqueous extract of *Aloe vera* (L.) burm F. (liliaceae). Eur Chem Bull. 2013;2:471–6.

31. Singh A, Singh VK, Quraishi MA. Effect of fruit extracts of some environmentally benign green corrosion inhibitors on corrosion of mild steel in hydrochloric acid solution. J Mater Environ Sci. 2010;1:162–74.

32. Deng S, Li X. Inhibition by Ginkgo leaves extract of the corrosion of steel in HCl and H$_2$SO$_4$ solutions. Corros Sci. 2012;55:407–15.

33. Samide A, Tutunaru B, Ionescu C, Tigae C, Moanţa A. Electrochemical study of haematoxylin inhibitory activity to control carbon steel corrosion in natrium nitrate solution. Int J Electrochem Sci. 2013;8:3589–601.

34. Yaro AS, Khadom AA, Wael RK. Apricot juice as green corrosion inhibitor of mild steel in phosphoric acid. Alex Eng J. 2013;52:129–35.

35. Souza FS, Spinelli A. Caffeic acid as a green corrosion inhibitor for mild steel. Corros Sci. 2009;51:642–9.

36. Eddy NO, Ibok UJ, Ebenso EE, El Nemr A, El Ashry ESH. Quantum chemical study of the inhibition of the corrosion of mild steel in H$_2$SO$_4$ by some antibiotics. J Mol Mod. 2009;15:1085–92.

37. Abdallah M. Antibacterial drugs as corrosion inhibitors for corrosion of aluminium in hydrochloric acid solution. Corros Sci. 2004;46:1981–96.

38. Shukla SK, Quraishi MA. Cefalexin drug: a new and efficient corrosion inhibitor for mild steel in hydrochloric acid solution. Mater Chem Phys. 2010;120:142–7.

39. Pang XH, Guo WJ, Li WH, Xie JD, Hou BR. Electrochemical, quantum chemical and SEM investigation of the inhibiting effect and mechanism of ciprofloxacin, norfloxacin and ofloxacin on the corrosion for mild steel in hydrochloric acid. Sci China Ser B-Chem. 2008;51:928–36.

40. Pang X, Ran X, Kuang F, Xie J, Hou B. Inhibiting effect of ciprofloxacin, norfloxacin and ofloxacin on corrosion of mild steel in hydrochloric acid. Chin J Chem Eng. 2010;18:337–45.

41. Shukla SK, Quraishi MA. The effects of pharmaceutically active compound doxycycline on the corrosion of mild steel in hydrochloric acid solution. Corros Sci. 2010;52:314–21.

42. Eddy NO, Odoemelam SA, Ogoko EC, Ita BI. Inhibition of the corrosion of zinc in 0.01–0.04 M H$_2$SO$_4$ by erythromycin. Port Electrochim Acta. 2010;28:15–26.

43. Samide A, Tutunaru B, Negrila C, Trandafir I, Maxut A. Effect of sulfacetamide on the composition of corrosion products formed onto carbon steel surface in hydrochloric acid. Dig J Nanomater Bios. 2011;6:663–73.

44. Shukla SK, Singh AK, Ahamad I, Quraishi MA. Streptomycin: a commercially available drug as corrosion inhibitor for mild steel in hydrochloric acid solution. Mater Lett. 2009;63:819–22.

45. Šnircová S, Jóna E, Janík R, Lajdová L, Lendvayová S, Loduhová M, Šutinská V, Durný R, Lizák P, Mojumdar SC. Co(II)-exchanged montmorillonite with ethylenediamine, trimethyl- and tetramethyl-ethylenediamine and their thermal decomposition. J Therm Anal Calorim. 2011;104:937–41.

46. Rejitha RS, Mathew S. Thermal behaviour of nickel(II) sulphate, nitrate and halide complexes containing ammine and ethylenediamine as ligands. J Therm Anal Calorim. 2011;106:267–75.

47. Wesołowski M, Szynkaruk P. Thermal decomposition of purine derivatives used in medicine. J Therm Anal Calorim. 2001;65:599–605.

48. Wesołowski M, Szynkaruk P. Thermal decomposition of methylxanthines. J Therm Anal Calorim. 2008;93:739–46.

49. Bán M, Bombicz P, Madarász J. Thermal stability and structure of a new co-crystal of theophylline formed with phthalic acid. J Therm Anal Calorim. 2009;95:895–901.

50. Fouda AS, Mostafa HA, El-Abbasy HM. Antibacterial drugs as inhibitors for the corrosion of stainless steel type 304 in HCl solution. J Appl Electrochem. 2010;40:163–73.

51. Zerga B, Attayibat A, Sfaira M, Taleb M, Hammouti B, Touhami ME, Radi S, Rais Z. Effect of some tripodal bipyrazolic compounds on C38 steel corrosion in hydrochloric acid solution. J Appl Electrochem. 2010;40:1575–82.

52. Samide A. A pharmaceutical product as corrosion inhibitor for carbon steel in acidic environments. J Environ Sci Health A Tox Hazard Subst Environ Eng. 2013;48:159–65.

53. Samide A, Tutunaru B. Corrosion inhibition of carbon steel in hydrochloric acid solution using a sulfa drug. Chem Biochem Eng Q. 2011;25:299–308.

54. Castro E, Víctor Mosquera V, Issa Katime I. Dual drug release of triamterene and aminophylline from poly(*N*-isopropylacrylamide) hydrogels. Nanomater Nanotechnol. 2012;2:Art. 6.

55. Zerga B, Hammouti B, Ebn Touhami M, Touir R, Taleb M, Sfaira M, Bennajeh M, Forssal I. Comparative inhibition study of new synthesised pyridazine derivatives towards mild steel corrosion in hydrochloric acid. Part-II: thermodynamic proprieties. Int J Electrochem Sci. 2012;7:471–83.

56. Ikpi ME, Udoh II, Okafor PC, Ekpe UJ, Ebenso EE. Corrosion inhibition and adsorption behaviour of extracts from *Piper guineensis* on mild steel corrosion in acid media. Int J Electrochem Sci. 2012;7:12193–206.

57. Wolkenstein Th. Physico-chimie de la surface des semi-conducteurs. Moscou: Editions Mir; 1977.

58. Paoletti P. Formation of metal complexes with ethylenediamine: a critical survey of equilibrium constants, enthalpy and entropy values. Pure Appl Chem. 1984;56:491–522.

59. Shaker SA, Farina Y. Co(II), Ni(II), Cu(II), Zn(II) and Cd(II) mixed ligand complexes of theophylline and cyanate: synthesis and spectroscopic characterization. Modern Appl Sci. 2009;3:88–93.